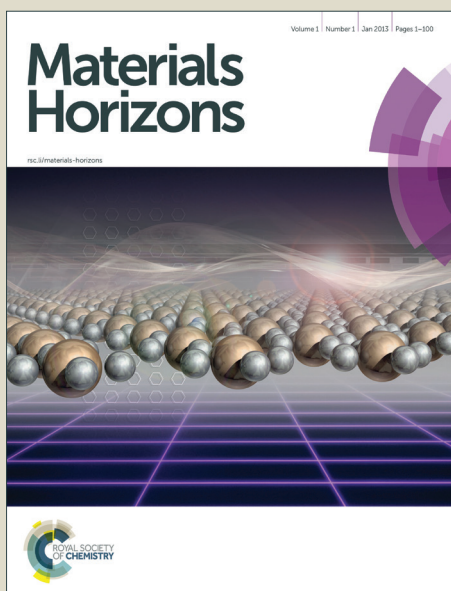


# Materials Horizons

Accepted Manuscript



This is an *Accepted Manuscript*, which has been through the Royal Society of Chemistry peer review process and has been accepted for publication.

*Accepted Manuscripts* are published online shortly after acceptance, before technical editing, formatting and proof reading. Using this free service, authors can make their results available to the community, in citable form, before we publish the edited article. We will replace this *Accepted Manuscript* with the edited and formatted *Advance Article* as soon as it is available.

You can find more information about *Accepted Manuscripts* in the [Information for Authors](#).

Please note that technical editing may introduce minor changes to the text and/or graphics, which may alter content. The journal's standard [Terms & Conditions](#) and the [Ethical guidelines](#) still apply. In no event shall the Royal Society of Chemistry be held responsible for any errors or omissions in this *Accepted Manuscript* or any consequences arising from the use of any information it contains.

## Conceptual Insights

Assemblies of organic-inorganic nanoparticles remains a frontier area of research for the development of optoelectronic, photovoltaic and light harvesting. Here, we have designed assemblies where QDs will absorb the visible light as an antenna material, followed by funneling of the exciton to an acceptor molecule which is confined in polymer nanoparticles. To design an assembly, polymer nanoparticles are surface functionalized by ionic liquid and then these nanoparticles are attached with negatively charged QDs. We investigate the efficient energy transfer from QDs to dye molecule inside polymer nanoparticles by using steady state and time resolved spectroscopy. Fundamental investigations of this resonance energy transfer from surface to the core centre of the assemblies will open up new possibilities for designing inorganic-organic assemblies for artificial light harvesting systems.

# Photoinduced Energy Transfer in Dye Encapsulated Polymer Nanoparticle - CdTe Quantum Dot Light-Harvesting Assemblies

Simanta Kundu, Santanu Bhattacharyya and Amitava Patra\*

Department of Materials Science, Indian Association for the Cultivation of Science,  
Kolkata 700 032, India

\*To whom correspondence should be addressed. E-mail: [msap@iacs.res.in](mailto:msap@iacs.res.in) Phone: (91)-33-2473-4971, Fax: (91)-33-2473-2805

### Abstract

Here, we have designed organic-inorganic light-harvesting assemblies where highly efficient resonance energy transfer occurs from CdTe QD (donor) to Nile Red dye (acceptor) encapsulated polymer nanoparticles. Our motivation is to develop an assembly where QDs will absorb the visible light as an antenna material, followed by funneling of the exciton to an acceptor molecule (Nile red) which is confined in polymer nanoparticles in order to enhance their energy transfer efficiency. Ionic liquid is being used to prepare positively charged Nile red (NR) dye encapsulated poly(methyl methacrylate) (PMMA) polymer nanoparticles. Then, negatively charged thioglycolic acid capped CdTe QDs are attached with the surface of polymer nanoparticles by electrostatic interaction. The drastic quenching of photoluminescence (60%) and the shortening of decay time of CdTe QD imply an efficient energy transfer (73%) from CdTe QD to the NR dye doped PMMA nanoparticles. Time resolved anisotropy decay measurement unravels the rotational motion of the dye molecules inside the PMMA nanoparticles. Interesting findings reveal that the efficient energy transfer in organic-inorganic assemblies may open up new possibilities in designing of artificial light harvesting system for future applications.

**Introduction:**

Self-assembled molecules, especially DNA conjugated system<sup>1-3</sup> and supra-molecular organization of conjugated molecules/fluorophores, dendrimers, organo gels etc.<sup>4-12</sup> are found to be most promising efficient light absorbing antenna materials. Emphasis has been given towards the light harvesting device fabrication by incorporation of fluorophore molecules inside confined matrix for better stability, functionality and aggregation free molecular arrangement.<sup>13, 14</sup> Attempts have been made to design a system where both the donor-acceptor fluorophore molecules are incorporated inside mesoporous silica.<sup>15-17</sup> Quenching due to self aggregation is the major limitation in this type of light harvesting devices. Furthermore, polymer nanoparticles are found to be an efficient host matrix for enhancing excitation energy transfer process from self organized donor to acceptor molecules.<sup>18, 19</sup> Dye doped organic/polymer fluorescent nanoparticles may be suitable as an acceptor system because the hydrophobic dyes are easily incorporated and dispersed within the hydrophobic polymer nanoparticles.<sup>20, 21</sup> Recent research focus has enlightened the dye doped polymer nanoparticles as an alternative luminescent source because of several outstanding features, i.e. easy synthetic procedure, easy to functionalize the surface, higher photostability, efficient brightness and color tunability.<sup>21-23</sup> Extensive investigation on photophysics of encapsulated dye molecules in polymer nanoparticles and their dependence on confined motions, matrix rigidity, and heterogeneous population have been reported very recently.<sup>21, 24</sup> Near-infrared fluorescent dye-doped semiconducting polymer dots are found to have efficient light harvesting application.<sup>25</sup>

In search of a light absorbing material, it is now well established that inorganic nanocrystals or quantum dots (QDs) are very useful for enhancing the light harvesting process, as they can absorb light over a wide spectral window.<sup>26, 27</sup> Semiconducting quantum dots are very fascinating because of their size dependent photophysical properties and photostability compared to conventional dyes.<sup>28, 29</sup> Particularly, variable sized quantum dots with tunable band gap energies have received significant attention for efficient solar light energy harvesting system<sup>30</sup> because visible light is effectively absorbed by QDs, followed by funneling of the excitation energy to a reaction center. Extensive work has been progress on QD based energy transfer for various applications.<sup>31-36</sup> However, the energy should be transferred in a unidirectional way for the light harvesting applications. In this regard, the energy transfer from

QDs to metal-organic framework or aggregated molecules is reported for enhancing light harvesting.<sup>37, 38</sup> Considering this concept, our idea is to design inorganic-organic conjugate system where QDs will absorb the visible light as an antenna material, and then transfer the exciton to an acceptor molecule which is confined in polymer nanoparticles.

To design polymer-inorganic assemblies, the surface functionalization of polymer nanoparticles is essential. The polymer nanoparticle surface becomes negatively charged when prepared by reprecipitation method due to formation of defects.<sup>39</sup> To overcome this, few studies have already done on the functionalization of the polymer nanoparticles. Recently, Chiu and his coworkers have functionalized the hydrophobic nanoparticles negatively by carboxylic groups.<sup>25, 40</sup> Here, we have used long tail 1-hexadecyl 3-methyl imidazolium bromide ionic liquid (IL) for the one step preparation and functionalization of Nile Red (NR) dye doped poly(methyl methacrylate) (PMMA) polymer (structures are shown in scheme 1) nanoparticles by simple reprecipitation method. The negatively charged CdTe QDs is being prepared by using thioglycolic acid (TGA). Finally, positively functionalized PMMA nanoparticles are then attached with TGA capped CdTe quantum dots. We investigate the efficient energy transfer from CdTe QDs to Nile red dye inside PMMA polymer nanoparticles by using steady state and time resolved spectroscopy. Fluorescence anisotropy decay study is also used to understand the energy migration. Fundamental investigations of this FRET based exciton energy accumulation from surface to the core centre of this composite nanostructure will open up new possibilities for designing inorganic-organic assemblies for artificial light harvesting systems.

## **Experimental Procedures:**

### **Preparation of ionic liquid**

The ionic liquid 1-hexadecyl-3-methylimidazolium bromide ([HDMIm]Br) was prepared by a reported method<sup>41, 42</sup> using microwave irradiation in a mixture of 1-methyl imidazole (Aldrich) and 1-Bromohexadecane (SRL). The prepared IL was then purified by recrystallization and dried in a vacuum. IL was characterized by NMR (<sup>1</sup>H and COSY) spectroscopy and ESI mass spectroscopy which are shown in the supporting information (Figure S1, S2 and S3) and the data's are well agreed with the previously reported values. Before using the IL, it was dried under high vacuum at 60° C to evaporate adsorbed water.

**Synthesis of IL functionalized Nile Red (NR) doped PMMA Nanoparticle:**

Positively charged PMMA polymer nanoparticles in water were prepared by using a very simple reprecipitation method.<sup>43</sup> In brief, 200  $\mu$ l of 4mg/ml PMMA polymer in THF (Merck), the required amount of NR (Aldrich) solution of fixed absorbance in THF and desired amount of 1mg/ml solution of synthesized IL in THF was mixed to a final volume of 1ml. Then, this mixed THF solution was rapidly injected to 20 ml of de-ionized water and vigorously stirred for 5 minutes. This solution was then sonicated for 3 minutes and the THF was evaporated in partial vacuum at 60<sup>0</sup>C for two hours. Thus, IL functionalized NR doped PMMA nanoparticle was prepared which are stable for more than a month. We have prepared different sets of NR doped PMMA nanoparticles with different IL concentrations to standardized the amount of IL. We have also prepared PMMA nanoparticles with final NR concentrations of 0.11  $\mu$ M, 0.22  $\mu$ M, 0.44  $\mu$ M, 0.66  $\mu$ M and 0.88  $\mu$ M in the nanoparticle solution with fixed IL concentration of 12.5  $\mu$ M.

**Synthesis of water soluble TGA capped CdTe QD:**

CdTe QD solution was synthesized using the reaction between CdCl<sub>2</sub> and NaHTe solution following reported methods with some modification.<sup>44, 45</sup> At first, NaHTe was prepared by adding 0.53 mM of NaBH<sub>4</sub> (Merck) and 0.18 mM of Te powder (Aldrich) in a round bottom flask, containing 2 mL of MilliQ water in N<sub>2</sub> atmosphere. On the other hand 0.10 mM of CdCl<sub>2</sub>.2.5H<sub>2</sub>O (Aldrich) was dissolved in 25 mL of MilliQ water. Then, 0.24 mM of Thioglycolic acid (Merck) was added to the solution and a white precipitate appears. The pH of the mixture was adjusted to 8-9 by adding required amount of NaOH which gives a clear solution. The mixture was bubbled by N<sub>2</sub> for 45 minutes to make O<sub>2</sub> free. Then, 0.06 mM of NaHTe was immediately injected into this mixture under vigorous stirring for 30 mins followed by refluxing at 110<sup>0</sup>C in aerial atmosphere. The reaction was quenched after 30 min of growth time and the resulting colloid was collected. These nanocrystals are stable for more than three months when we stored at 10<sup>0</sup>C.

**Preparation of NR encapsulated PMMA polymer nanoparticle - CdTe QD assemblies:**

The required amount of CdTe QD solution was added to the synthesized IL modified polymer nanoparticle solution under mild sonication. The final concentrations of TGA capped CdTe QD in the conjugate solutions were fixed to 1  $\mu$ M. The negatively charged TGA capped CdTe QDs are attached with positively charged IL functionalized polymer nanoparticle surface

by electrostatic interaction. The pH of the final solution becomes 6.5. All the solutions were kept for 5 hours at room temperature for stabilization before the characterization.

### Characterization:

NMR spectroscopy study of the ionic liquid was carried out by using a Bruker DPX 500 MHz spectrometer. The ESI mass spectrum of the ionic liquid was recorded from a methanol solution in a Quadrupole time-of-flight (Qtof) Micro YA263 mass spectrometer. Morphological studies of the polymer nanoparticles were done by a field emission scanning electron microscope (FESEM, JEOL, JSM - 6700F). Detailed structural features of QD and conjugate solutions were investigated by a high-resolution transmission electron microscopy (HRTEM; JEOL 2010). Zeta potential was measured in Malveron Zetasizer instrument. Room temperature optical absorption spectra were taken by a UV-vis spectrophotometer (SHIMADZU). Room temperature photoluminescence studies were carried out by using a Fluoro Max – P (Horiba Jobin Yvon) luminescence spectrometer. For the time-correlated single-photon-counting (TCSPC) measurements, the samples were excited at 375 and 489 nm using picoseconds NANO-LED IBH 375L and picoseconds NANO-LED IBH 489 equipments. The TCSPC measurement of the NR was performed by excitation with 375 nm wavelength generated from a 750 nm Ti-sapphire laser pulse of 80 MHz and decay time was measured by a Halcyone lifetime measurement system. Equation (1) was used to analyze the experimental time-resolved fluorescence decays,  $P(t)$ :

$$P(t) = b + \sum_i^n \alpha_i \exp(-t/\tau_i) \quad (1)$$

Here,  $n$  is the number of emissive species,  $b$  is the baseline correction (“dc” offset), and  $\alpha_i$  and  $\tau_i$  are, respectively, the pre-exponential factor and the excited-state fluorescence lifetime associated with the  $i^{\text{th}}$  component. The average lifetime,  $\langle \tau \rangle$ , was calculated from Equation (2):

$$\langle \tau \rangle = \sum_{i=1}^n a_i \tau_i \quad (2)$$

Where  $a_i = \alpha_i / \sum \alpha_i$  and is the contribution of the decay component.

For anisotropy decays, we used a motorized polarizer in the emission side. The analyzer was rotated by  $90^\circ$  at regular intervals. The parallel ( $I_{\parallel}$ ) and perpendicular ( $I_{\perp}$ ) polarizations were collected alternatively until a certain peak difference between parallel ( $I_{\parallel}$ ) and perpendicular decays were reached. The  $r(t)$  value was calculated by the following formula:



$$r(t) = \frac{I_{\parallel}(t) - GI_{\perp}(t)}{I_{\parallel}(t) + 2GI_{\perp}(t)} \quad (3)$$

The analysis of the time resolved data was done using IBH DAS, version 6 decay analysis software. The same software was used to analyze the anisotropy data. All the experiments were done at room temperature.

## Results and Discussion

During the synthesis of polymer nanoparticles by re-precipitation method, THF solution of PMMA was injected into water and THF quickly diffuses in the water and as a result nanoparticles are formed by coiling of PMMA polymer chains. These nanoparticles are negatively charged due to formation of defects. To functionalize the surface of nanoparticles with +ve charge, we used 1-hexadecyl 3-methyl imidazolium bromide ionic liquid (IL). When IL was added during re-precipitation, the long hydrophobic tail of the IL grafted in the PMMA nanoparticle leaving the +ve imidazole group in the outer surface of the nanoparticles. Thus, positively functionalized polymer nanoparticles are successfully prepared by using IL in single step. FESEM is being used to investigate the morphology and particle size and figure 1a shows the SEM image of the NR doped PMMA nanoparticles with IL concentrations of 12.5  $\mu\text{M}$ . It can be seen from the SEM image that the particles are spherical in nature with an average diameter of 50 ( $\pm 10$ ) nm. The SEM images of the polymer nanoparticles with IL concentration 6.25  $\mu\text{M}$  and 25  $\mu\text{M}$  are shown in the supporting information (figure S4). It is observed from size distribution plot (figure S5) that particle size of the polymer nanoparticles increases with increasing the IL concentration. Zeta potential of these three nanoparticles were measured and the zeta potentials were found to be +13.2 mV, +20.2 mV and +38.7mv for 6.25  $\mu\text{M}$ , 12.5  $\mu\text{M}$  and 25  $\mu\text{M}$  concentration of IL, respectively, indicating the IL concentration controls the surface charge of the particles. It is also observed that there is no change in the absorption spectra of the solvatochromic NR dye inside polymer nanoparticle due to functionalization (figure S6), which confirms that IL has no influence on dye environment in dye encapsulated polymer nanoparticles. The encapsulation of the NR inside the polymer nanoparticles has been confirmed from the emission spectra of the NR. Figure 1b shows the PL spectra of NR dye encapsulated PMMA nanoparticle and NR dye in water. The PL intensity at 640 nm is very low in water after

excitation at 530 nm, but the PL intensity enhances drastically and shifts to 600 nm when encapsulated within PMMA due to the change of polarity due to encapsulation within polymer. When the NR dyes get encapsulated within the hydrophobic domain of the polymer nanoparticles, a drastic change in the dye environment occurs from polar to nonpolar environment. Thus this blue shifting of the NR emission indicates that dye molecules are encapsulated in the hydrophobic PMMA nanoparticles.<sup>24</sup> No significant change in PL intensity of NR emission with changing the concentration from 6.25 to 25  $\mu\text{M}$  IL (see supporting information figure S7). It reveals that the IL has no significant influence on the encapsulated dye within the PMMA, indicating that the IL molecules are on the surface of the nanoparticles.

TGA capped CdTe QD exhibits an absorption band at 470 nm and PL band at 520 nm after excitation at 375 nm (figure S8a). The quantum yield of the CdTe solution is 3.5%. The average diameter of the CdTe nanoparticles is found to be  $\sim 2.4$  nm from the TEM image (figure S8b and S8c). As the nanoparticles are capped with thioglycolic acid (TGA), the zeta potential of the CdTe nanoparticle is  $-38.2\text{mV}$ . Thus, the negatively charged CdTe nanoparticles are added to positively charged dye doped PMMA nanoparticle solution for preparing assemblies. The synthesis pathway of the conjugate is summarized in scheme 2. It can be seen from TEM image of CdTe QD - IL functionalized PMMA nanoparticle assemblies (figure S9) that the CdTe nanoparticles are attached with the surface of the polymer nanoparticles.

Figure 2A shows the absorption spectra of CdTe QD solution, NR doped ( $0.44 \mu\text{M}$ ) PMMA polymer solution, conjugate solution and the mixture of QD and polymer nanoparticle solutions without IL functionalization. The absorption spectrum of assemblies exhibit both NR and CdTe absorption peaks (plot c). No shifting of the peak position is observed after attachment of QD with the polymer nanoparticle. Inset of figure 2A shows the photograph of the solutions without illumination of light. Under 365 nm illumination, CdTe solution shows a bright green emission, and NR doped PMMA solution exhibits red color. But, the QD-NR doped PMMA conjugates exhibit a bright yellow emission (inset of figure 2B). After the attachment of the CdTe QD with the IL functionalized NR doped polymer nanoparticle, the quenching of the CdTe emission is observed. Figure 2B shows the emission spectrum of the QD, NR doped polymer nanoparticle, NR doped PMMA polymer - QD conjugates and a mixture of QD and NR doped polymer nanoparticle without IL functionalization at 375 nm excitation. From the figure 2B, it is

seen that the emission band of CdTe QD at 520 nm decreases after attachment with the NR doped PMMA nanoparticle, whereas the intensity of the NR emission (plot b) enhances drastically after the attachment (plot c). No such effect is observed when we have mixed the CdTe nanoparticle solution with the NR doped PMMA nanoparticle without functionalization with IL. Instead, the intensity of the CdTe fluorescence slightly enhances (plot d) which may be due to the repulsion with the negatively charged PMMA nanoparticles and thus enhancing the fluorescence. Thus, we may say that IL plays a crucial role for preparing conjugate system.

The enhancement of the NR emission and decrease of the CdTe emission in the composite system suggests that there might be some energy transfer process from the outer CdTe nanoparticles to the NR dye confined inside the PMMA polymer. It is interesting to note that there is an overlap between the absorption spectra of the NR inside PMMA with the emission spectra of the CdTe nanoparticle solution. Figure 3 shows the overlap between the emission of the donor CdTe nanocrystal and the absorption of the acceptor NR molecule inside PMMA. The spectral overlap  $J(\lambda)$ <sup>46</sup> between the emission spectrum of donor and absorption of acceptor is given by equation:

$$J(\lambda) = \frac{\int_0^{\infty} F(\lambda)\varepsilon(\lambda)\lambda^4 d\lambda}{\int_0^{\infty} F(\lambda)d\lambda} \quad (4)$$

where  $F(\lambda)$  represents the emission intensity of donor at a wavelength  $\lambda$ , and  $\varepsilon(\lambda)$  is the molar absorption coefficient of acceptor. The overlap integral is found to be  $3.06 \times 10^{15} \text{ M}^{-1}\text{cm}^{-1}\text{nm}^4$ . Thus, there is a very good overlap between the emission spectra of the donor CdTe and absorption of the acceptor NR molecule inside the PMMA matrix. Therefore, an energy transfer process occurs from the outside CdTe molecule to NR molecules inside polymer nanoparticles. For further understanding and confirmation of the energy transfer process from CdTe to NR encapsulated polymer nanoparticles, we have performed systematic studies by varying the concentration of the acceptor NR concentration inside the PMMA nanoparticle (figure 4A). It can be observed that the emission of CdTe quenches gradually and the emission of NR increases with increasing the acceptor NR concentration within the PMMA nanoparticle at 375 nm excitation. The PL intensity of NR inside PMMA is very low at 375 nm excitation (plot b Figure

3B). Thus, the enhanced PL intensity of acceptor (NR) is due to energy transfer only which is discussed further by measuring the decay time of acceptor. The PL quenching efficiencies vary from 18% to 60% with changing the concentration from 0.11  $\mu\text{M}$  to 0.88  $\mu\text{M}$ . This quenching of CdTe emission occurs due to energy transfer process and that can proceed via radiative or nonradiative pathway. To understand the energy transfer process more clearly, we have measured the decay times of pure CdTe and conjugate system with increasing NR concentration (figure 4B). The decay profiles are well fitted with tri-exponentials. It can be seen that the decay times of the CdTe QD decreases gradually with the increase of NR concentration within the attached PMMA nanoparticles. The average decay time of CdTe QD is found to be 11.08 ns. The average decay time decreases to 8.62 ns, 6.51 ns, 5.39 ns, 4.16 ns and 2.99 ns after the attachment with 0.11, 0.22, 0.44, 0.66 and 0.88  $\mu\text{M}$  NR doped PMMA nanoparticles, respectively. The decay time parameters are summarize in Table 1. The decay time of CdTe QD decreases with increasing the acceptor concentration, which suggests that the energy transfer occurs via nonradiative pathway from CdTe to NR molecule inside PMMA. The energy transfer efficiency can be calculated by using the following equation:

$$\phi_{\text{ET}} = 1 - \tau_{\text{DA}}/\tau_{\text{D}} \quad (5)$$

where  $\tau_{\text{DA}}$  and  $\tau_{\text{D}}$  are the average decay times of the conjugate solution and pure CdTe QD, respectively. The energy transfer efficiency from CdTe to 0.88  $\mu\text{M}$  NR doped PMMA nanoparticle is found to be 73%. Again, we have measured the fluorescence lifetime of the acceptor NR molecule inside PMMA monitoring at 600 nm, before and after attachment with the CdTe QD (figure 5) at the excitation wavelength of 375 nm. It is found that the decay time of the NR molecule increases from 2.38 ns to 3.14 ns. This enhancement of the lifetime of the acceptor molecule also confirms the energy transfer process.

Time resolved anisotropy decay measurement is being used to understand the rotational motion of the dye molecules inside the PMMA nanoparticles. The motions of the dye molecules become restricted when NR molecule is encapsulated inside the polymer nanoparticles, which controls the photophysical behavior of encapsulated dye molecules. We have previously reported the restricted motions of the encapsulated dye molecules inside polymer matrix.<sup>24</sup> As the polymer nanoparticles are large in size compare to the dye molecule, the rotational time of the nanoparticles are comparatively large (in  $\mu\text{s}$  time scale). Thus, the Brownian motion of the

nanoparticles does not affect the rotational motion of the encapsulated dye molecules inside the polymer nanoparticles. We have measured the fluorescence anisotropy decay of the NR emission in the CdTe attached polymer nanoparticle (NR concentration 0.44  $\mu\text{M}$ ) solution at 489 nm i.e. direct excitation of NR and 375 nm i.e. at CdTe excitation (figure 6). Fluorescence anisotropy decay is fitted with a bi-exponential function:

$$r(t) = r_0 \left[ a \exp\left(-\frac{t}{\tau_{slow}}\right) + (1-a) \exp\left(-\frac{t}{\tau_{fast}}\right) \right] \quad (6)$$

here,  $\tau_{slow}$  and  $\tau_{fast}$  are the two reorientation times associated with the slow and fast motions of NR dye in PMMA polymer nanoparticles. 'a' is the pre-exponential factor which indicates the relative contributions of the slow and fast motions to the anisotropy decay. The average reorientation time  $\langle \tau_r \rangle$  can be expressed as

$$\langle \tau_r \rangle = a \tau_{slow} + (1-a) \tau_{fast} \quad (7)$$

At direct excitation of NR (489 nm), the fluorescence anisotropy decay is polarized due to restricted motion of the NR molecules inside PMMA matrix and the  $r(0)$  value is found to be 0.325. The average reorientation time is 3.15 ns with a faster component of 0.91 ns (65%) and a slow component of 7.32 ns (35%). When we monitor the fluorescence anisotropy decay of the NR at the CdTe QD excitation (375 nm), the reduction of the anisotropy confirms the depolarization of NR emission. In this case, the  $r(0)$  value is found to be 0.13 and the average reorientation time is 0.64 ns with a faster component of 0.48 ns (93%) and a slow component of 3.25 ns (7%). This depolarization occurs due to the energy transfer from surface CdTe QD to randomly distributed NR molecules inside PMMA nanoparticles.<sup>47</sup> It reveals that the efficient energy transfer takes place from QD to NR molecules inside the polymer nanoparticles. This energy migration from the surface to the centre of a nanoparticle can open up new possibilities for light harvesting applications.

## Conclusion

We have successfully demonstrated the preparation of dye encapsulated polymer nanoparticles-CdTe QDs assemblies by attaching positively surface charged polymer nanoparticles using ionic liquid with negatively charged QDs. QDs are used as the antenna

materials and they rapidly energy transfer to dye molecules, encapsulated into polymer nanoparticles. Steady state and time resolved spectroscopic studies confirm the energy transfer from QD to Nile red dye. Time resolved anisotropy measurement shows the depolarization of the NR emission inside the PMMA nanoparticles via energy transfer pathway. Thus, this IL functionalized dye doped polymer NP and QD hybrid nanostructure can open up new possibilities in designing the light harvesting nanostructures for future applications.

**Acknowledgement:**

SERB (DST) and Indo-Spain (DST) are gratefully acknowledged for financial support. SK thanks CSIR and SB thanks IACS for awarding fellowship.

† **Electronic Supplementary Information (ESI) available:** NMR (proton and COSY) and mass spectra of the IL, SEM images of the NR doped PMMA nanoparticles with IL concentration of 6.25  $\mu\text{M}$  and 25  $\mu\text{M}$ , Size distribution plot of the PMMA nanoparticles with different IL concentrations, absorption spectra of the NR encapsulated in PMMA nanoparticles with and without functionalization by IL, emission spectra of the NR doped PMMA nanoparticle at the excitation of 525 nm without IL functionalization and with increasing concentration of the IL, normalized absorption and emission spectra of TGA capped CdTe nanocrystals, TEM image of the as prepared TGA capped CdTe nanocrystals in water, TEM image of assemblies]. See DOI: 10.1039/b000000x/

**References:**

1. J. G. Woller, J. K. Hannestad and B. Albinsson, *J. Am. Chem. Soc.*, 2013, **135**, 2759-2768.
2. P. K. Dutta, R. Varghese, J. Nangreave, S. Lin, H. Yan and Y. Liu, *J. Am. Chem. Soc.*, 2011, **133**, 11985-11993.
3. G. Jiang, A. S. Susa, A. A. Lutich, F. D. Stefani, J. Feldmann and A. L. Rogach, *ACS nano*, 2009, **3**, 4127-4131.
4. T. Ishi-i, K.-i. Murakami, Y. Imai and S. Mataka, *Org. Lett.*, 2005, **7**, 3175-3178.
5. K. Sugiyasu, N. Fujita and S. Shinkai, *Angew. Chem.*, 2004, **116**, 1249-1253.
6. A. Ajayaghosh, V. K. Praveen and C. Vijayakumar, *Chem. Soc. Rev.*, 2008, **37**, 109-122.
7. A. Adronov and J. M. J. Frechet, *Chem. Commun.*, 2000, 1701-1710.
8. N. Nishiyama, H. R. Stapert, G.-D. Zhang, D. Takasu, D.-L. Jiang, T. Nagano, T. Aida and K. Kataoka, *Bioconjug. Chem.*, 2003, **14**, 58-66.
9. K. V. Rao, K. K. R. Datta, M. Eswaramoorthy and S. J. George, *Chem. -Euro. J.*, 2012, **18**, 2184-2194.
10. A. Adronov, S. L. Gilat, J. M. J. Fréchet, K. Ohta, F. V. R. Neuwahl and G. R. Fleming, *J. Am. Chem. Soc.*, 2000, **122**, 1175-1185.
11. A. Ajayaghosh, S. J. George and V. K. Praveen, *Angew. Chem. Int. Ed.*, 2003, **42**, 332-335.
12. M. Cotlet, T. Vosch, S. Habuchi, T. Weil, K. Müllen, J. Hofkens and F. De Schryver, *J. Am. Chem. Soc.*, 2005, **127**, 9760-9768.
13. T. Sen, S. Jana, S. Koner and A. Patra, *J. Phys. Chem. C*, 2009, **114**, 707-714.
14. C. N. Fleming, P. Jang, T. J. Meyer and J. M. Papanikolas, *J. Phys. Chem. B*, 2004, **108**, 2205-2209.
15. N. Kameta, K. Ishikawa, M. Masuda, M. Asakawa and T. Shimizu, *Chem. Mater.*, 2012, **24**, 209-214.
16. G. Calzaferri, *Langmuir*, 2012, **28**, 6216-6231.
17. G. Calzaferri, S. Huber, H. Maas and C. Minkowski, *Angew. Chem. Int. Ed.*, 2003, **42**, 3732-3758.
18. Z. Tian, J. Yu, C. Wu, C. Szymanski and J. McNeill, *Nanoscale*, 2010, **2**, 1999-2011.

19. C. Martin, S. Bhattacharyya, A. Patra and A. Douhal, *Photochem. Photobiol. Sci.*, 2014, **13**, 1241-1252.
20. E. J. Harbron, C. M. Davis, J. K. Campbell, R. M. Allred, M. T. Kovary and N. J. Economou, *J. Phys. Chem. C*, 2009, **113**, 13707-13714.
21. C. Wu, Y. Zheng, C. Szymanski and J. McNeill, *J. Phys. Chem. C*, 2008, **112**, 1772-1781.
22. S. Bhattacharyya, S. Prashanthi, P. R. Bangal and A. Patra, *J. Phys. Chem. C*, 2013, **117**, 26750-26759.
23. Z. Tian, J. Yu, X. Wang, L. C. Groff, J. L. Grimland and J. D. McNeill, *J. Phys. Chem. B*, 2012, **117**, 4517-4520.
24. S. Bhattacharyya, B. Paramanik and A. Patra, *J. Phys. Chem. C*, 2011, **115**, 20832-20839.
25. Y. Jin, F. Ye, M. Zeigler, C. Wu and D. T. Chiu, *ACS nano*, 2011, **5**, 1468-1475.
26. A. O. Govorov, *Adv. Mater.*, 2008, **20**, 4330-4335.
27. I. Robel, V. Subramanian, M. Kuno and P. V. Kamat, *J. Am. Chem. Soc.*, 2006, **128**, 2385-2393.
28. X. Michalet, F. F. Pinaud, L. A. Bentolila, J. M. Tsay, S. Doose, J. J. Li, G. Sundaresan, A. M. Wu, S. S. Gambhir and S. Weiss, *Science*, 2005, **307**, 538-544.
29. U. Resch-Genger, M. Grabolle, S. Cavaliere-Jaricot, R. Nitschke and T. Nann, *Nat. Meth.*, 2008, **5**, 763-775.
30. A. Makhal, H. Yan, P. Lemmens and S. K. Pal, *J. Phys. Chem. C*, 2009, **114**, 627-632.
31. I. L. Medintz and H. Mattoussi, *Phys. Chem. Chem. Phys.*, 2009, **11**, 17-45.
32. R. Wargnier, A. V. Baranov, V. G. Maslov, V. Stsiapura, M. Artemyev, M. Pluot, A. Sukhanova and I. Nabiev, *Nano lett.*, 2004, **4**, 451-457.
33. S. Sadhu, K. K. Haldar and A. Patra, *J. Phys. Chem. C*, 2010, **114**, 3891-3897.
34. J. Ji, L. He, Y. Shen, P. Hu, X. Li, L.-P. Jiang, J.-R. Zhang, L. Li and J.-J. Zhu, *Anal. Chem.*, 2014, **86**, 3284-3290.
35. A. C. S. Samia, S. Dayal and C. Burda, *Photochem. Photobiol.*, 2006, **82**, 617-625.
36. E. R. Goldman, I. L. Medintz, J. L. Whitley, A. Hayhurst, A. R. Clapp, H. T. Uyeda, J. R. Deschamps, M. E. Lassman and H. Mattoussi, *J. Am. Chem. Soc.*, 2005, **127**, 6744-6751.
37. S. Jin, H.-J. Son, O. K. Farha, G. P. Wiederrecht and J. T. Hupp, *J. Am. Chem. Soc.*, 2013, **135**, 955-958.



38. B. J. Walker, V. Bulović and M. G. Bawendi, *Nano lett.*, 2010, **10**, 3995-3999.
39. S. N. Clifton, D. A. Beattie, A. Mierczynska-Vasilev, R. G. Acres, A. C. Morgan and T. W. Kee, *Langmuir*, 2010, **26**, 17785-17789.
40. C. Wu, T. Schneider, M. Zeigler, J. Yu, P. G. Schiro, D. R. Burnham, J. D. McNeill and D. T. Chiu, *J. Am. Chem. Soc.*, 2010, **132**, 15410-15417.
41. R. S. Varma and V. V. Namboodiri, *Chem. Commun.*, 2001, 643-644.
42. S. Kundu, A. Kar and A. Patra, *J. Lumin.*, 2012, **132**, 1400-1406.
43. D. Tuncel and H. V. Demir, *Nanoscale*, 2010, **2**, 484-494.
44. A. L. Rogach, T. Franzl, T. A. Klar, J. Feldmann, N. Gaponik, V. Lesnyak, A. Shavel, A. Eychmüller, Y. P. Rakovich and J. F. Donegan, *J. Phys. Chem. C*, 2007, **111**, 14628-14637.
45. S. Kundu, S. Sadhu, R. Bera, B. Paramanik and A. Patra, *J. Phys. Chem. C*, 2013, **117**, 23987-23995.
46. J. R. Lakowicz, *Principles of fluorescence spectroscopy, 3rd ed.*, 2006, **XXVI**, 954 p.
47. M. N. Berberan-Santos and B. Valeur, *J. Chem. Phys.*, 1991, **95**, 8048-8055.

## Figure Captions

**Scheme 1.** Chemical structures of (A) PMMA polymer, (B) Nile red dye and (C) ionic liquid.

**Figure 1.** (a) SEM image of the NR doped PMMA nanoparticles with IL concentration of 12.5  $\mu\text{M}$ , (b) emission spectra of NR in water in presence of IL (i) and within IL functionalized PMMA polymer nanoparticles (ii).

**Scheme 2.** Schematic representation of the synthesis of the QD- IL functionalized NR doped PMMA nanoparticle assemblies.

**Figure 2.** (A) UV spectra of the CdTe nanoparticle solution in water (a), IL functionalized NR doped PMMA nanoparticle solution in water (b), and polymer-QD conjugate solution (c), mixture solution of CdTe and NR doped PMMA nanoparticles without IL functionalization (d), inset shows the photograph of the solutions at room light, (B) Photoluminescence spectra of the CdTe nanoparticle solution in water (a), IL functionalized NR doped PMMA nanoparticle solution in water (b), PMMA nanoparticles- QDs assemblies (c) and mixture solution of CdTe and NR doped PMMA nanoparticles without IL functionalization (d) at 375 nm excitation, inset photograph shows the corresponding solutions under 365 nm UV torch light.

**Figure 3.** The overlap plot between the emission spectrum of CdTe nanoparticle solution and the absorption spectrum of the IL functionalized NR doped PMMA nanoparticle solution.

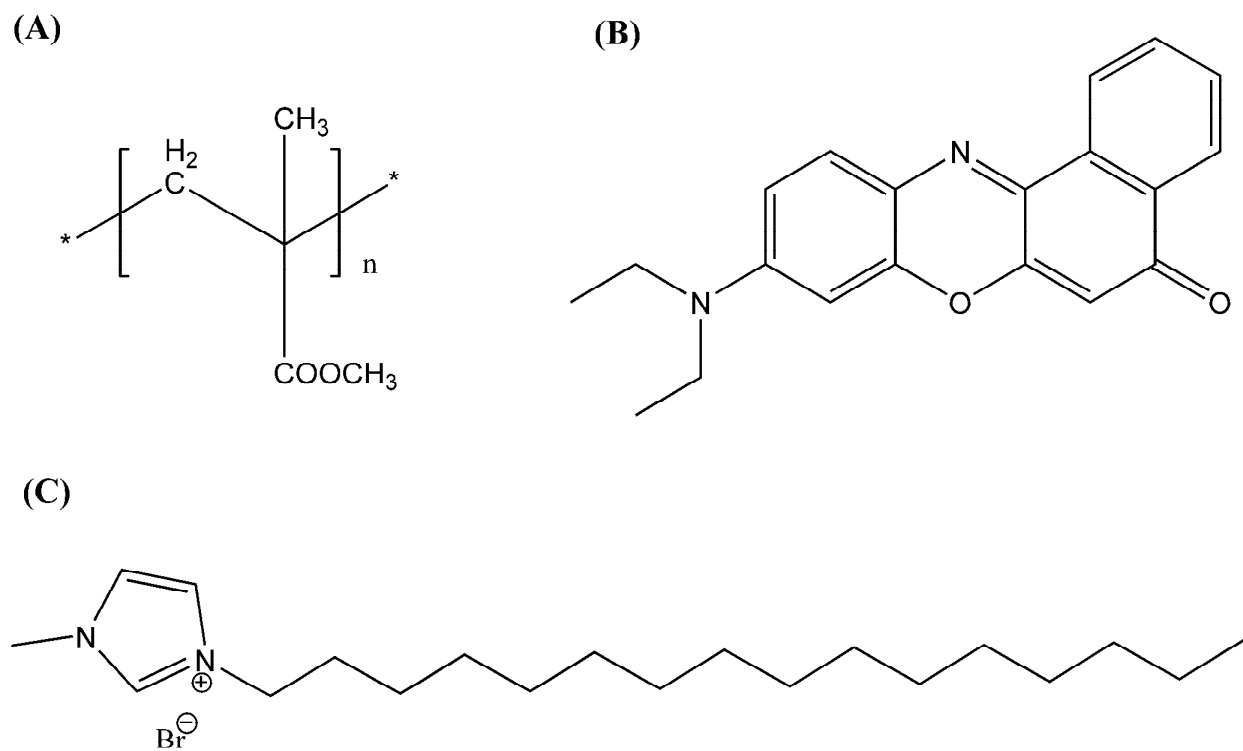
**Figure 4.** (A) Photoluminescence spectra of the CdTe nanoparticle (a) and with NR concentration of (b) 0.11  $\mu\text{M}$ , (c) 0.22  $\mu\text{M}$ , (d) 0.44  $\mu\text{M}$ , (e) 0.66  $\mu\text{M}$  and (f) 0.88  $\mu\text{M}$  within the PMMA nanoparticle of the hybrid solution, (B) Time-resolved decay time plots of the CdTe nanoparticle (a) and with NR concentration of (b) 0.11  $\mu\text{M}$ , (c) 0.22  $\mu\text{M}$ , (d) 0.44  $\mu\text{M}$ , (e) 0.66  $\mu\text{M}$  and (f) 0.88  $\mu\text{M}$  within the PMMA nanoparticle of assemblies.

**Figure 5.** Decay time plot of the NR dye inside IL functionalized NR doped PMMA nanoparticles (a) before and after (b) the attachment with CdTe QD at the excitation of 375 nm and the emission monitored at 600 nm.

**Figure 6.** Time-resolved anisotropy decay curves of assemblies monitored at 600 nm at the excitation of (a) 489 nm and (b) 375 nm.

**Table 1:** Decay time parameters of CdTe QD with increase of NR concentration within PMMA nanoparticles.

Concentration of NR	$\tau_1$ (ns) ( $\alpha_1$ )	$\tau_2$ (ns) ( $\alpha_2$ )	$\tau_3$ (ns) ( $\alpha_3$ )	$\langle\tau\rangle$ (ns)
Pure CdTe	2.23 (0.36)	10.89 (0.48)	31.55 (0.16)	11.08
0.11 $\mu\text{M}$	1.21 (0.42)	8.33 (0.43)	30.20 (0.15)	8.62
0.22 $\mu\text{M}$	0.84 (0.45)	6.82 (0.43)	26.68 (0.12)	6.51
0.44 $\mu\text{M}$	0.82 (0.48)	6.03 (0.42)	24.66 (0.10)	5.39
0.66 $\mu\text{M}$	0.77 (0.55)	5.52 (0.38)	23.52 (0.07)	4.16
0.88 $\mu\text{M}$	0.56 (0.57)	4.22 (0.36)	19.21 (0.06)	2.99



**Scheme 1.** Chemical structures of (A) PMMA polymer, (B) Nile red dye and (C) ionic liquid 1-hexadecyl 3-methyl imidazolium bromide.

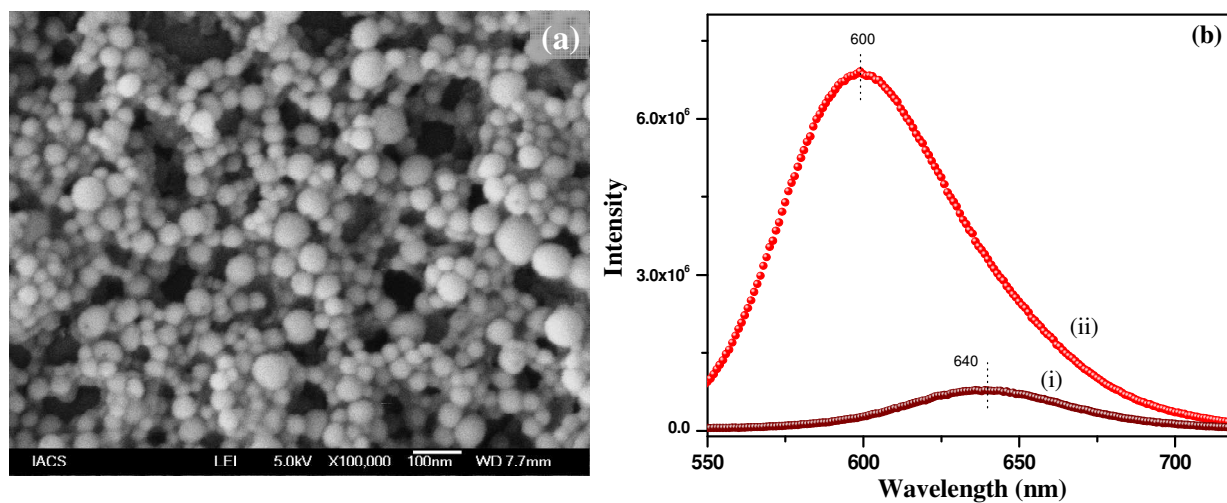
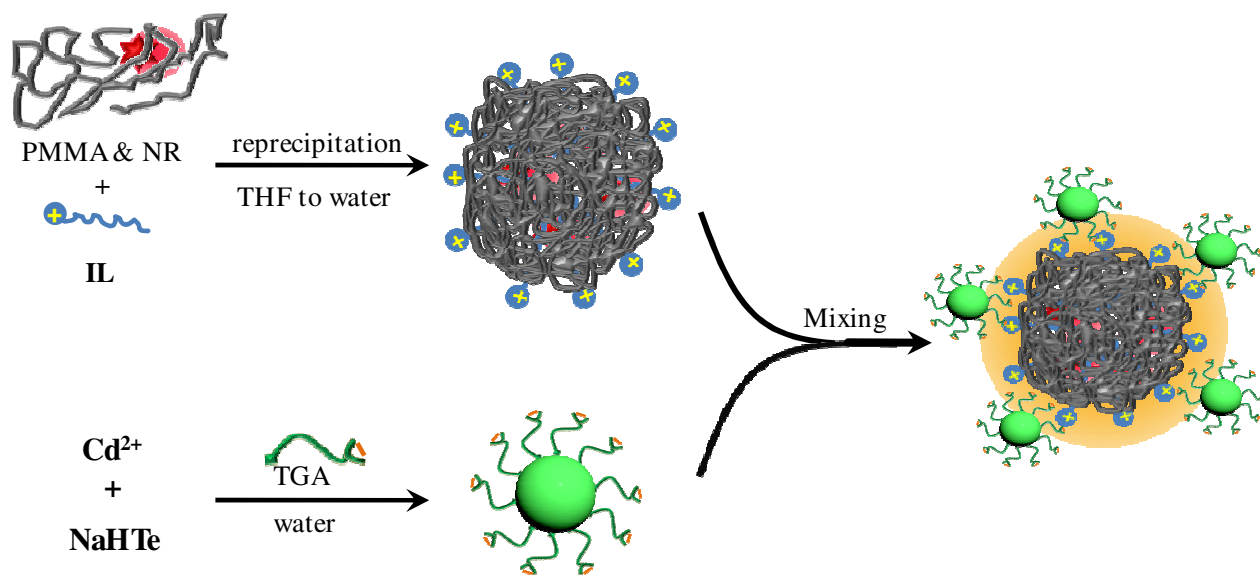


**Figure 1.** (a) SEM image of the NR doped PMMA nanoparticles with IL concentration of 12.5  $\mu\text{M}$ , (b) emission spectra of NR in water in presence of IL (i) and within IL functionalized PMMA polymer nanoparticles (ii).



**Scheme 2.** Schematic representation of the synthesis method of the QD- IL functionalized NR doped PMMA nanoparticle assemblies.

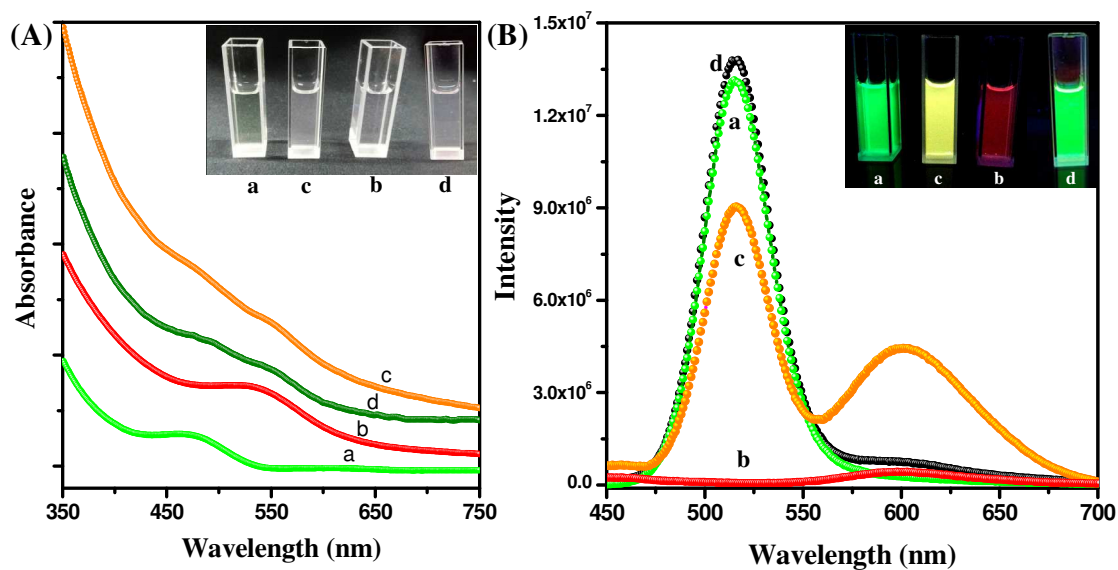


**Figure 2.** (A) UV spectra of the CdTe nanoparticle solution in water (a), IL functionalized NR doped PMMA nanoparticle solution in water (b), and polymer-QD conjugate solution (c), mixture solution of CdTe and NR doped PMMA nanoparticles without IL functionalization (d), inset shows the photograph of the solutions at room light, (B) Photoluminescence spectra of the CdTe nanoparticle solution in water (a), IL functionalized NR doped PMMA nanoparticle solution in water (b), PMMA nanoparticles- QDs assemblies (c) and mixture solution of CdTe and NR doped PMMA nanoparticles without IL functionalization (d) at 375 nm excitation, inset photograph shows the corresponding solutions under 365 nm UV torch light.

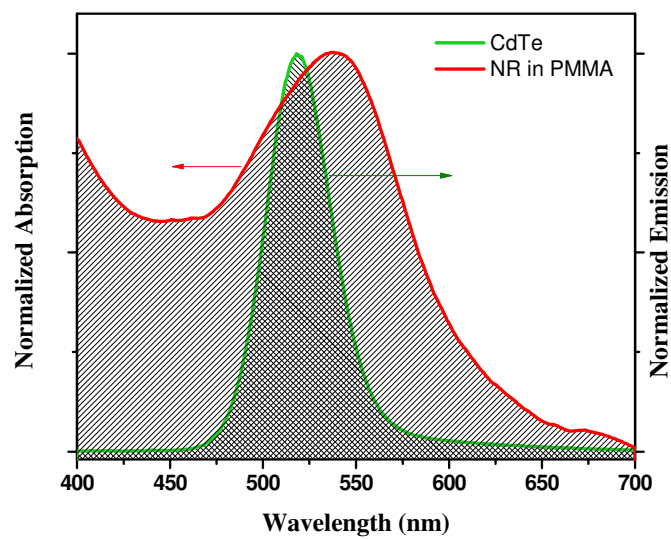


**Figure 3.** The overlap plot between the emission of CdTe nanoparticle solution and the absorption spectrum of the IL functionalized NR doped PMMA nanoparticle solution.



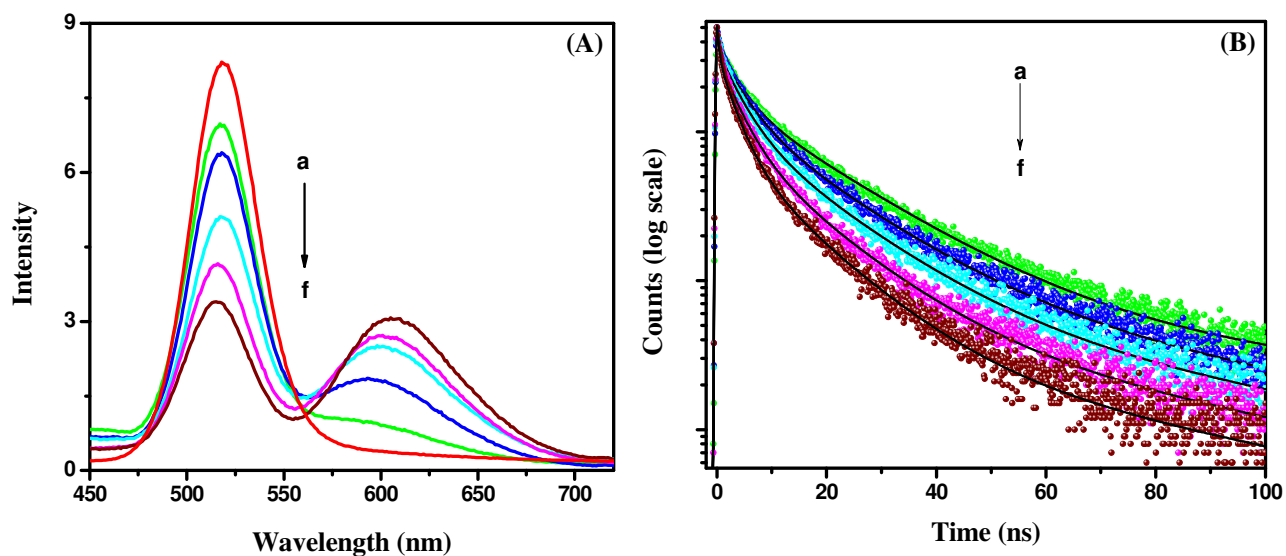


**Figure 4.** (A) Fluorescence spectra of the CdTe nanoparticle (a) and with NR concentration of (b) 0.11  $\mu\text{M}$ , (c) 0.22  $\mu\text{M}$ , (d) 0.44  $\mu\text{M}$ , (e) 0.66  $\mu\text{M}$  and (f) 0.88  $\mu\text{M}$  within the PMMA nanoparticle of the hybrid solution, (B) Time-resolved decay time plots of the CdTe nanoparticle (a) and with NR concentration of (b) 0.11  $\mu\text{M}$ , (c) 0.22  $\mu\text{M}$ , (d) 0.44  $\mu\text{M}$ , (e) 0.66  $\mu\text{M}$  and (f) 0.88  $\mu\text{M}$  within the PMMA nanoparticle of assemblies.

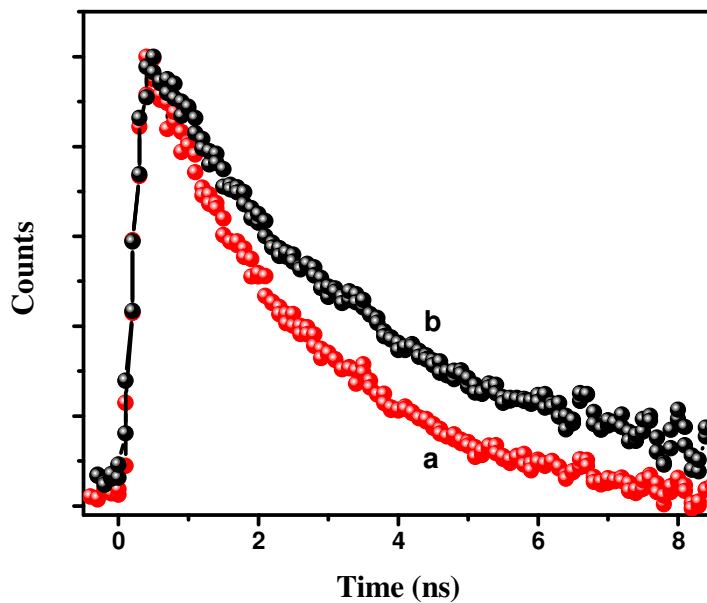


**Figure 5.** Decay time plots of the NR dye inside IL functionalized NR doped PMMA nanoparticles (a) before and after (b) the attachment with CdTe QD at the excitation of 375 nm and the emission monitored at 600 nm.

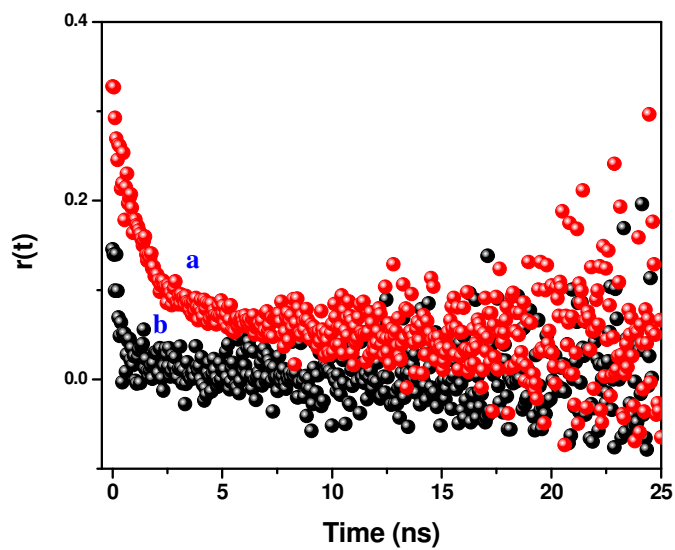
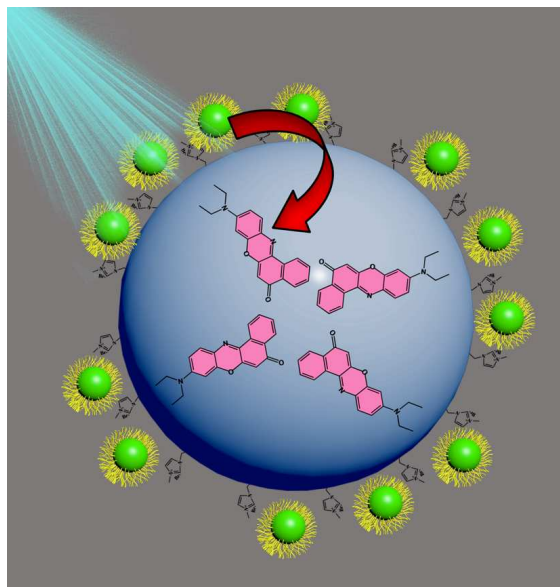


**Figure 6.** Time-resolved anisotropy decay curves of assemblies monitored at 600 nm at the excitation of (a) 489 nm and (b) 375 nm.

**Graphical Abstract**

Efficient resonance energy transfer from CdTe QD (donor) to Dye (acceptor) encapsulated PMMA nanoparticles for light harvesting



**Graphical Abstract**

Efficient resonance energy transfer from CdTe QD (donor) to Dye (acceptor) encapsulated PMMA nanoparticles for light harvesting

